Lehigh University
Lehigh Preserve

Fritz Laboratory Reports

Civil and Environmental Engineering

1957

Rotation capacity of a three span continuous beam, Lehigh University, 1957

G. C. Driscoll Jr.

Interim Report No. 34

ROTATION CAPACITY
of a
THREE-SPAN CONTINUOUS BEAM

by

George C. Driscoll, Jr.

This work has been carried out as a part of an investigation sponsored jointly by the Welding Research Council and the Department of the Navy with funds furnished by the following:

American Institute of Steel Construction
American Iron and Steel Institute
Institute of Research, Lehigh University
Office of Naval Research (Contract Nonr 610(03))
Bureau of Ships
Bureau of Yards and Docks

Fritz Engineering Laboratory
Department of Civil Engineering
Lehigh University
Bethlehem, Pennsylvania

June, 1957

Fritz Laboratory Report No. 268.2

(Not for Publication)

TABLE OF CONTENTS

A B S T R A C T

Plastic analysis of steel structures depends on the ability of the members to form plastic hinges and to redistribute moments. In order for redistribution of moment to take place, certain plastic hinges must sustain their plastic moment through some angle of rotation. The amount of rotation required may affect the stability of the structure and, therefore, may affect the geometry of the structural shapes selected and the spacing of lateral bracing. The ability of a structural member to rotate the required amount in order to redistribute the necessary moments and form a mechanism is defined as the "rotation capacity". The angle of rotation during which a yielded segment of beam must sustain its plastic moment value is termed the "hinge angle".

This paper deals with a method of calculating the approximate hinge angle through which a member must be able to rotate to form a mechanism.

The presentation is made only to indicate the method of solving such a problem and therefore is restricted to the case of a symmetrical three-span beam of constant cross section.

1. INTRODUCTION

Recent developments in the plastic analysis of steel structures have presented a more rational basis on which to design welded continuous structures. Methods based on these developments give promise of economies to be gained by taking advantage of the reserve of strength of structural steel beyond the elastic limit, by using simple methods of analysis, and by assuring a uniform factor of safety against failure for all structures.[1]

Plastic analysis supplements the classic elastic theory by utilizing knowledge of the behavior of structural steel beyond the elastic limit. It is known that the same property of ductility which allows the deformation without additional load of a tension or compression member, will also allow a flexural member, stressed to a limiting moment (designated as the plastic hinge moment) to bend or rotate without additional moment. The ability of a plastic hinge to maintain a constant moment while rotating through a finite angle allows a structure or member to transfer additional increasing load to other less-stressed portions of the structure until sufficient plastic hinges have formed to cause the structure or a portion thereof to become a mechanism. These two properties are known as the plastification of cross section, and redistribution of moment. While plastification of cross section and redistribution of moment are the two primary factors involved in the plastic analysis of structures, certain other factors affect plastic behavior, and at times can govern the plastic analysis or design. Axial compressive forces and shear forces combined with bending moment tend to reduce the plastic hinge moment of a given structural member. However, axial loads less than 15% of the compressive yield load of a member, as are most common in rigid portal frames, reduce the plastic hinge moment only a small amount and may be neglected.[1] The usual shear forces in a normal balanced design are also small enough so that the plastic moment is not seriously reduced. When the shear forces are large, they occur in a section of steep moment gradient which generally allows strain hardening to produce a counteracting effect.[3]

The presence of residual stresses due to cooling, welding or cold bending tends to reduce the yield load of a structure. In a compression member, the maximum load is thus reduced, but in a member subjected to bending only, the predicted plastic hinge moment is generally achieved.[12]

The former factors affect the magnitude of the plastic hinge moment but have little influence on the ability of the member to absorb plastic rotations. Other factors may affect not only the plastic hinge moments but also the ability of the section to rotate thus modifying the redistribution of moment. These other factors are brittle fracture, local buckling and lateral buckling. In structures which have thus far been investigated, brittle fracture has not proved to be of concern because careful welding procedures and inspection, and the use of satisfactory materials for the temperatures encountered prevented brittle behavior.[2] The occurrence of premature local buckling can be prevented by selecting shapes of the proper geometric proportions.[4,5] Lateral buckling may also be delayed by providing proper bracing to the members.[11] It is evident, then, that proper attention must be paid to the possibility of brittle fracture, local buckling, and lateral buckling to assure sufficient strain or rotation to permit redistribution of moment.

There is no single answer as to how much strain or rotation of a plastic hinge is required to allow a mechanism to form. The attainment of strain hardening has arbitrarily been selected as a criterion in the previously mentioned studies on local and lateral buckling. The ability of a plastic hinge to rotate at or near the maximum moment has been defined as rotation capacity.[10]

This paper will present methods of calculating the rotation capacity required to allow a mechanism to form in a structure and will give results for some specific cases. The object of the study is actually two-fold--one aim is to discover methods of calculating the rotations which must be sustained for the calculated maximim load to be attained. The second aim is to determine if some maximum amount of required rotation capacity may be specified for given geometrical and loading conditions which will not be exceeded in any structure so that a design rule may be set up eliminating the necessity of calculating the required rotations. The latter goal is desirable because the calculation of deflections and rotations for even the simplest of structures is tedious and to be avoided if at all possible. Essentially the problem of calculating the required rotation capacity is one of calculating the deformation at ultimate load. This problem may be examined as if it were broken into three distinct steps:

(1) Calculation of the ultimate load and ultimate moment diagram.

(2) Location of the first and last plastic hinges to be formed in the structure.

(3) Calculation of deflection and rotation by solving the differential equation for the curvature of bending members considering boundary conditions appropriate for a structure in the plastic range.

2. DETERMINATION OF MOMENTS AT MAXIMUM LOAD

A number of available methods of analysis use the properties of plastification of cross section and redistribution of moment as a basis for calculating the ultimate loads of structures.[1,7,8] An important advantage of these methods of plastic analysis over methods of elastic analysis is the elimination of the solution of large numbers of simultaneous equations in the analysis of highly indeterminate structures. Instead, orderly procedures may be used to calculate the ultimate loads consistent with various assumed mechanisms. Each such load constitutes an upper bound for the true maximum load of the structure. At the same time, any assumed set of loads and redundants which satisfy equilibrium without the plastic hinge moment being exceeded at any point in the structure constitutes a lower bound for the true maximum load of the structure. The exact maximum load is indicated when an upper bound and a lower bound prove to be equal.

Consider the three-span continuous beam shown in Fig. 1. The main span has a length L and is flanked by two side spans of length βL. A uniformly distributed load w pounds per foot is applied to the main span, and a load of αw pounds per foot to the side spans. The cross section and material are constant throughout.

Since the relative loads and span lengths are undetermined as stated, the mode of failure cannot be uniquely defined. It is possible for a mechanism to form either in the main span or in the side spans.

If a mechanism is to form in the main span, plastic hinges will form at the interior supports and at the center of the main span. For this case, an elementary calculation will give as the expression relating the plastic hinge moment of the beam and the maximum load:

$$M_p = \frac{wL^2}{16} \tag{1}$$

If a mechanism is to form in the side span, plastic hinges will form at the interior supports and at an intermediate point having the largest moment in each side span. The distance from the exterior support to each of these hinges will be some fraction ζ of the side span length βL, i.e. $\zeta\beta L$. The plastic hinge moment in this case is given by the expression:

$$M_p = \alpha\beta^2 \frac{wL^2}{2} \frac{\zeta(1-\zeta)}{(1+\zeta)}$$

where $\zeta = \sqrt{2} - 1 = 0.4142$.

then $$M_p = \frac{1}{11.66} \alpha\beta^2 wL^2 \tag{2}$$

For a given beam section, side span length and side span loading, the mechanism which would require the greater value of M_p will occur. A special condition is that in which both mechanisms occur simultaneously. For this case, both expressions for M_p must be equal. By combining equations (1) and (2) an expression for the values of α and β for which both mechanisms can form is obtained.

$$\alpha\beta^2 = \frac{1}{8} \frac{(1+\zeta)}{\zeta(1-\zeta)} \tag{3}$$

By substituting for δ its value 0.4142, this equation reduces to:

$$\alpha \beta^2 = 0.728 \tag{4}$$

This curve is plotted in Fig. 2.

The unshaded area of Fig.2 contains all values of α and β for which the mechanism will form in the main span with a plastic hinge moment given by equation (1). The shaded area contains the values of α and β for which the mechanism will form simultaneously in the two side spans and the plastic hinge moment will be given by Eq. (2).

3. LOCATION OF LAST PLASTIC HINGE

As was stated earlier, the boundary conditions used in calculating deflection and rotation in the plastic range depend on the location of the last plastic hinge. One way of determining the location of the last plastic hinge is to calculate step-by-step the load versus moment behavior of the structure starting with an elastic solution.

In the case of the three-span beam, one step is sufficient because only two hinges are necessary to form a mechanism (because of symmetry the two hinges at the interior supports count as one hinge). Thus, locating the first hinge by an elastic solution gives the location of the last hinge by elimination.

From an elastic analysis of the beam, the following moments may be obtained:

Maximum Moment in Main Span

$$M_E = \frac{wL^2}{4}\left[\frac{1}{2} - \frac{\alpha\beta^3+1}{2\beta+3}\right] \tag{5}$$

Moment at Interior Supports

$$M_B = \frac{wL^2}{4}\left[\frac{\alpha\beta^3+1}{2\beta+3}\right] \tag{6}$$

Maximum Moment in Side Span

$$M_F = \frac{wL^2}{32\alpha\beta^2}\left[\frac{3\alpha\beta^3+6\alpha\beta^2-1}{2\beta+3}\right]^2 \tag{7}$$

For a given loading and span length, one of these moments will prove to be the largest and, therefore, the first plastic hinge would occur at that location. The sizes of the moments should be considered in pairs consistent with the two types of possible mechanism. Thus, for the main span mechanism, the question of interest is whether or not M_B is greater than M_E. For the side span mechanism, M_B and M_F should be compared.

When M_B and M_E are equated, the resulting expression in α and β gives the boundary between the regions where the first plastic hinge forms at B and at E.

$$\frac{\beta + 1.5}{\alpha\beta^3 + 1} = 2 \tag{8}$$

This curve is plotted as the lower curve in Fig. 3. The region below the curve designates the values of α and β for which the maximum elastic moment is at the center of the main span E. The region above the curve designates α and β for maximum elastic moment at the interior supports B.

Similarly, equating M_B and M_F results in an equation separating the regions for maximum elastic moment at B and F.

$$\frac{(3\alpha\beta^3 + 6\alpha\beta^2 - 1)^2}{\alpha\beta^2(2\beta + 3)(\alpha\beta^3 + 1)} = 8 \tag{9}$$

This curve is plotted as the upper curve in Fig. 3. Within the region enclosed by the curve, the maximum elastic moment occurs at F. Below the curve the maximum elastic moment occurs at point B.

As an approximation, the limiting value of the elastic moment may be considered as the plastic hinge moment. Thus, the three areas in Fig. 3 indicate the values of α and β for which each of the three possible plastic hinges are first to form.

By superimposing Fig. 2 on Fig. 3, a single chart (Fig. 4) is obtained which indicates both the type of mechanism and the location of the first plastic hinge. This information by elimination also gives the location of the last plastic hinge, providing all the information needed to deduce boundary conditions.

The method used in this case for the determination of the order of formation of plastic hinges is the simplest form of the step-by-step method. However, for a highly indeterminate structure, the step-by-step method would require a complete elastic solution of the structure for each plastic hinge that forms.

Fortunately there exists a method of calculation which uses only the maximum load moment diagram to determine the last plastic hinge.[7,1] This method consists of assuming any given plastic hinge to be the last to form and making a deflection calculation based on this assumption. This calculation is repeated with as many "last plastic hinge" assumptions as there are uncertainties as to its true location. The true last plastic hinge corresponds to the greatest calculated deflection.

4. BEHAVIOR OF STRUCTURE IN FORMING MECHANISM

Before making an actual calculation of the rotations of this beam, it may be helpful to visualize the behavior of the beam in the forming of a mechanism under the action of steadily increasing proportional loads.

For example, consider a case when α equals 0.5 and β equals 1.0. From Fig. 4 it is seen that in this case a main span mechanism would form with the first plastic hinge at the interior supports.

The actual moment-curvature behavior of a typical wide-flange shape such as might be used for this beam is shown diagrammatically in Fig. 5a. This curve exhibits the effects of the elastic range, the gradual transition from yielding in the flanges to the complete plastic hinge, residual stresses, and the effect of strain hardening as has been fully discussed in literature on the subject of plastic behavior.

For the purpose of simplification of calculations, assumptions of behavior in an idealized manner will be used in the development here. The material in the beam will be assumed as a ductile material having the idealized stress-strain curve shown in Fig. 5b, i.e., strain-hardening and the upper yield point will be neglected. As a further assumption, the M-ϕ curve will be used in the idealized form shown in Fig. 5c. As well as the assumptions of the idealized stress-strain curve, this curve neglects residual stresses and the gradual transition from elastic to fully plastic behavior.

In the first phase of the formation of the mechanism, the complete beam would be elastic. The deflected shape of the beam would be a fully continuous smooth curve. The shape of the elastic curve over support B would be as shown in Fig. 6a. Note that the slope at the joint is the same in each span. The load-deflection curve for the beam in the phase would be as shown digramatically by curve I in Fig. 7a and 7b. Increasing the loads until the maximum moment at B reached M_p would cause a plastic hinge to form at that point. In this condition, the curvature ϕ of point B would not be uniquely determined by the moment. The curvature could be the equivalent of point A in Fig. 5c, in which case the beam would look like Fig. 6a. at the joint, or the curvature could be the equivalent of any other point on line AB in Fig. 5c. Then the beam would have a discontinuity at the joint as in Fig. 6b. In a case like this, the slope at the joint is not the same in each span. Since the amount of discontinuity is not uniquely determined by the moment at the hinge, it must be governed by the behavior of other parts of the structure.

Because the three-span beam is an indeterminate structure, formation of the first plastic hinge would not create a mechanism. However, the formation of this plastic hinge would introduce a "known" moment into the picture, thereby removing the indeterminacy. (Because of symmetry, plastic hinges would form at the two interior supports simultaneously.) At this stage, the remainder of the length of the beam would still be bent in smooth curves, and the three spans could be considered as separate simple beams loaded as shown in Fig. 8. Except for local conditions caused by yielding at the supports, these spans would be piecewise continuous and satisfy the conditions which permit the slope and deflection to be calculated by standard elastic methods. Therefore, the end slopes at the interior supports could be calculated and the angle of discontinuity determined.

On increasing the loads proportionally, the changes in moments in the three spans would be those of simple beams, because the end moments M_p would remain constant. This is the phase of loading in which redistribution of moment takes place. The load-deflection curve due to this increment of loading would be as shown diagrammatically by curve II in Fig. 7. Eventually, the center of the main span would have its moment increased to M_p. Then the curvature ϕ at that point would be undefined as in the case of the first hinge. However, at the precise instant the moment reached M_p, the M-ϕ relationship would be the equivalent of point A in Fig. 5c. This stage in the behavior of a structure is very important because it is the last stage at which a solution may be obtained for the slope and deflection of the structure. It is also the stage at which the ultimate load of the structure has been reached. Considering the deflected shape of the beam at this same stage, it is apparent that the three spans would still be bent in smooth curves between the supports and that the spans would satisfy the conditions which allow slope and deflection to be calculated by elastic methods. This would permit the calculation of the hinge angle which is the main objective of this study. This critical hinge angle is the angle through which the first plastic hinge must rotate up to the instant that the last plastic hinge just begins to form. The importance of this angle is evident when it is realized that if the angle cannot be reached, the structure may not be able to carry the predicted ultimate load on which plastic design is based.

Although a structure plastically designed would not be required to deform further after formation of the last plastic hinge, consideration of its behavior in this range is worthwhile because it sheds some light on the virtual displacement method of determining ultimate load.

Up to the instant that the last plastic hinge formed in the middle of the main span, the curve of the beam would be smooth as in Fig. 9a. This is the boundary condition which makes possible the determination of slope and deflection of the beam. Once the last hinge formed, its rotation could increase without addition of load and a hinge angle would be evident as shown in Fig. 9b.. It would not be possible to calculate the hinge angles since the structure would now be overdeterminate and subject to an infinite number of solutions for deflection and hinge rotations.

At this point it may be well to distinguish between the slope angles and hinge angles which have been discussed here and the mechanism angles which are used to determine the ultimate load of structures by the virtual displacement method.

The angles such as θ_{BC} and θ_{EB} shown in Fig. 6 and 9 are slopes to the "elastic" curve of the structure. The hinge angles such as H_B (Fig. 6b) are the differences in adjacent slopes at a point where a discontinuity has occurred due to formation of a plastic hinge. These slopes and angles have unique values up to the ultimate load.

In contrast, the mechanism angles (also designated as θ) are imaginary rotations of complete lengths of members resulting from imaginary controlled displacements of structures already at their ultimate load. Because the external loads and internal moments remain constant during these virtual displacements, internal and external work may be expressed simply as a function of load, M_p, geometry of the structure, and θ. Equating internal and external work from these expressions gives a value for load in terms of M_p and geometry of the structure with θ cancelling completely.

The physical picture of these angles will be shown with the aid of Fig. 10. Fig. 10a shows a typical method of describing the mechanism of the beam for the purpose of writing the virtual work equation. The beam, already at maximum load, has been subjected to a virtual displacement, Δ , causing virtual rotations θ at the interior supports, and 2 θ at the center plastic hinge. (Loads have been omitted to allow the angles to be seen more clearly.) In Fig. 10b is seen an enlarged view of the portion BE of the beam just before the virtual displacement was effected. The bent shape of all members is piecewise continuous between hinges. Because bending moments will remain constant throughout any displacement, the shape of each of these pieces will remain constant. This is just as if they were rigid curved links connecting the hinges at each end. Shown in Fig. 10b are the vertical deflection δ due to bending and the hinge angle H_B. In the condition indicated by the drawing, the beam would just be reaching maximum load and H_B would be the hinge angle required for maximum load. Fig. 10c shows the beam after the virtual displacement, Δ, has taken place. The rigid link BE has rotated on an amount θ and the added rotation at joint E is 2 θ.

The angles caused by the virtual displacement Δ are θ at joint B and 2 θ at joint E. These are superimposed on the hinge angles which were H_B at joint B and zero at joint E.

For the purpose of the virtual work equations, the virtual displacements are assumed to approach zero in order that they won't constitute a change in the geometry of the structure.

5. METHOD OF CALCULATING ROTATIONS AT MAXIMUM LOAD

Calculation of the deflections and rotations of flexural members at maximum load is accomplished by integration, with appropriate boundary conditions, of the differential equation:

$$\frac{d^2y}{dx^2} = \phi \tag{10}$$

where y = deflection from original straight line of member

x = distance along member

ϕ = curvature of member, a function of moment

Since ϕ is a function of moment and since the moment is a function of x, ϕ may be expressed as a function of x.

Next the question arises of the form of ϕ for use in this equation. ϕ could conceivably be used in a form which would represent the actual shape of the M-ϕ curve and could also include the effect of residual stresses and strain hardening. (Fig. 5a). However this would require the use of tedious calculation procedures and probably give answers which are not particularly more significant than those which can be derived using simplifying assumptions.[6] For the purpose of obtaining quickly a qualitative overall picture of the rotation capacity problem, the assumption of the idealized M-ϕ curve as shown in Fig. 5c will be made. By using this assumption, the function of ϕ along a member and between plastic hinges may be represented as M/EI just as in elastic analysis. This neglects only the area between the solid line and the dotted line and may be shown to have a small effect.[6]

By assuming ϕ equal to M/EI, it is possible to use all the methods of calculation of deflections of elastic analysis which use orderly procedures or evaluated integrals of the M/EI curve in the form of formulas and thus simplify mathematical operations. These methods include moment-area, conjugate beam, virtual work and slope deflection. The choice of method is generally governed by an individual's preference of an orderly form for calculations or an easily remembered sign convention. In the following solutions, slope-deflection equations will be used in the following form:[1,9]

$$\theta_N = \theta'_N + R_{NF} + \frac{l}{3EI}\left[M_{NF} - \frac{1}{2}M_{FN}\right] \qquad (11)$$

θ_N = Slope of near end of member

θ'_N = Slope of near end of similarly loaded member when simply supported = $\pm \dfrac{wl^3}{24EI}$

R_{NF} = Rotation of a chord between ends of member
= Deflection of one end of a member with respect to the other divided by the distance between them $= \delta/l$

l = Length of member or portion of member

M_{NF} = Moment at near end of member

M_{FN} = Moment at far end of member

Any of the sign conventions convenient for slope deflection may be used. The convention used here is that slope angles are defined as positive, when the rotations are clockwise, and end moments are defined as positive when acting in the clockwise sense.

θ is used to represent the slope on both sides of a point. H is used to represent the difference in slope at a plastic hinge at maximum load. See Fig. 6.

θ as used here is not the same as the virtual rotations used for calculating internal work due to virtual displacement of a mechanism. Once the bending moments for a structure are known, the slope deflection equations are used by writing an equation similar to (11) for each end of each member. The unknowns in these equations will be the θ and R terms (θ' are known). Additional equations will be needed to solve the problem. These may be derived by considering the compatibility of the R terms; i.e., the R rotations must be such that the members remain connected together at the joints. Solution of the unknown θ and R terms gives sufficient information for determining all deflections and the hinge angles at each plastic hinge.

6. DERIVATION OF EQUATIONS FOR HINGE ANGLES

Using the findings of sections 2, 3, and 4, it may be determined that there exist four possible cases of mechanism and order of formation of plastic hinges for the three-span continuous beam. Diagrams of these cases are shown in Fig. 11. Sketches singling out the boundary conditions and unknowns for each case are given in Fig. 12. Using these conditions, a hinge angle will be calculated for each case.

Case I. Main Span Mechanism--First Hinge at Midspan

For this case the plastic hinge moment is

$$M_p = \frac{wL^2}{16} \tag{12}$$

The boundary conditions are indicated in Fig. 12. Slope-deflection equations are to be written for lengths AB and BE with continuity assumed at joint B, the last plastic hinge. In span AB, the rotation at B is calculated as the end rotation of a uniformly loaded simple beam with a moment Mp applied at end B.

$$\theta_{BA} = -\frac{(\alpha w)(\beta L)^3}{24EI} + \frac{\beta L}{3EI}\left[M_p - \frac{1}{2}(0)\right] \tag{13}$$

In semi-span BE, the end rotation at B is:

$$\theta_{BE} = \frac{wL^3}{24(8)EI} + R_{BE} + \frac{\frac{L}{2}}{3EI}\left[-M_p + \frac{1}{2}M_p\right] \tag{14}$$

Since $\theta_{BE} = \theta_{BA}$,

$$R_{BE} = \frac{wL^3}{24EI}\left[-\alpha\beta^3 - \frac{1}{8}\right] + \frac{M_pL}{3EI}\left[\beta + \frac{1}{4}\right] \tag{15}$$

The end rotation at E is:

$$\theta_{EB} = \frac{-wL^3}{24(8)EI} + R_{BE} + \frac{\frac{L}{2}}{3EI}\left[-M_p + \frac{1}{2}M_p\right] \tag{16}$$

Substituting for R_{BE}:

$$\theta_{EB} = \frac{wL^3}{24EI}\left[-\frac{1}{4} - \alpha\beta^3\right] + \frac{M_pL}{3EI}\beta \tag{17}$$

By symmetry, the hinge angle, H_E, is twice θ_{EB}

$$H_E = \frac{wL^3}{24EI}\left[-\frac{1}{2} - 2\alpha\beta^3\right] + \frac{2}{3}\frac{M_pL}{EI}\beta \tag{18}$$

By use of equation (12) this equation may be expressed either in terms of Mp or w. Thus

$$\begin{aligned} H_E &= \frac{wL^3}{48EI}(2\beta - 1 - 4\alpha\beta^3) \\ &= \frac{M_pL}{3EI}(2\beta - 1 - 4\alpha\beta^3) \end{aligned} \tag{19}$$

Equation 19 may be written in the form

$$\frac{H_E}{\phi_p L} = \frac{2}{3}\beta - \frac{1}{3} - \frac{4}{3}\alpha\beta^3 \tag{20}$$

where

$$\phi_p = \frac{M_p}{EI} = \frac{wL^2}{16EI} \tag{21}$$

Equation 20 is plotted in non-dimensional form as a family of curves in Fig. 13b. Values of α and β for which Equation 20 is applicable are limited by the appropriate domain in Fig. 4. As plotted in Fig. 13b, all values of α and β satisfy this requirement.

Case II. Main Span Mechanism--First Hinge at Support B

Because the final mechanism is the same as Case I, the plastic hinge moment is

$$M_p = \frac{wL^2}{16}. \tag{22}$$

The critical angle is the hinge angle at interior support B. This is obtained by calculating the end slope of the simple beam AB with end moment Mp as for Case I and also calculating the end slope of simple beam BC with two end moments Mp (Fig. 12). The hinge angle is then the difference in slope.

$$\theta_{BA} = \frac{wL^3}{48EI}\left[\beta - 2\alpha\beta^3\right] = \frac{M_pL}{3EI}\left[\beta - 2\alpha\beta^3\right] \tag{23}$$

$$\theta_{BC} = \frac{1}{96}\frac{wL^3}{EI} = \frac{1}{6}\frac{M_pL}{EI} \tag{24}$$

$$H_B = \theta_{BC} - \theta_{BA} \tag{25}$$

$$H_B = \frac{wL^3}{96EI}\left[4\alpha\beta^3 - 2\beta + 1\right]$$

$$= \frac{M_pL}{EI}\left[\frac{2}{3}\alpha\beta^3 - \frac{1}{3}\beta + \frac{1}{6}\right] \tag{26}$$

The non-dimensional form of this equation is:

$$\frac{H_B}{\theta_p L} = \frac{2}{3}\alpha\beta^3 - \frac{1}{3}\beta + \frac{1}{6} \tag{27}$$

This equation is plotted as a family of curves in Fig. 13a. The values as plotted are consistent with the limits imposed on α and β for the main span mechanism with first hinge at the support (Fig. 4).

Case III. Side Span Mechanism--First Hinge at Support B

When the mechanism forms in the outer span, one hinge forms at the interior support and one forms at a point F at a distance $0.4142\beta L$ from the outer support A. Replacing ζ by its numerical value of 0.4142 in equation (2) gives:

$$M_p = \frac{1}{11.66}\alpha\beta^2 wL^2 \tag{28}$$

The controlling boundary condition in this case is that the beam remains continuous at point F until the mechanism has formed.

The hinge angle at B may be calculated from the end slopes of two simple beams having the given moment diagrams.

$$\theta_{BA} = -\frac{\alpha\beta^3 wL^3}{24EI} + \frac{M_p\beta L}{3EI}$$

$$\theta_{BC} = \frac{wL^3}{24EI} - \frac{M_pL}{2EI} \tag{29}$$

(30)

$$H_B = \frac{M_pL}{6EI}\left[0.915\beta - 3 + \frac{2.915}{\alpha\beta^2}\right]$$

(31)

In non-dimensional form, the equation for H_B is:

$$\frac{H_B}{\phi_p L} = 0.1524\beta - \frac{1}{2} + \frac{0.486}{\alpha\beta^2}$$

(32)

where

$$\phi_p = \frac{M_p}{EI} = \frac{\alpha\beta^2 wL^2}{11.66EI}$$

(33)

This case is plotted in Figure 14a.

Case IV. <u>Side Span Mechanism--First Hinge in Span at Section F</u>

In this case, the first hinge forms in the side span. Span BF is analyzed as an overhanging cantilever extending from simple span BC. Span AF is a simple span supported at one end by the original end support and at the other end by the cantilever span BF. The controlling boundary condition is continuity at point B, the position of the last plastic hinge.

The hinge angle for this case is:

$$\frac{H_F}{\theta_p L} = 0.368\beta - 1.207 + \frac{1.173}{\alpha\beta^2} \tag{34}$$

This is plotted in Fig. 14b. Since equation (16) is negative for all values of α and β for which it applies, the absolute value is plotted.

7. DISCUSSION

7.1 Illustrative Examples

a. General Example

The use of the charts can be illustrated by a simple example.

Given: Three equal spans, L= 30 ft.
Main span maximum load, 2k/ft.
Side span maximum load, 1k/ft.

Find: Rolled shape for the beam.
Hinge angle required to develop all necessary plastic hinges.

From the given data,

$$\alpha = 0.5$$

$$\beta = 1.0$$

Entering Fig. 4, it is found that this beam will form a main span mechanism with the first hinge at the supports.

Since $M_p = \dfrac{wL^2}{16}$ (Eq. 1)

then $$Z = \frac{M_p}{\sigma_y} = \frac{wL^2}{16\sigma_y}$$

$$= \frac{2 \times 30 \times 12 \times 30}{16 \times 33} = 40.8 \text{ in.}^3 \qquad (35)$$

A 14 WF 30 has a plastic section modulus of 47.1 in.^{3} and is the most economical section strong enough for this load.

Fig. 13a gives the hinge angle for a main span mechanism with first hinge at the interior support. For $\alpha = 0.5$ and $\beta = 1.0$

$$\frac{H_B}{\phi_p L} = 0.166 \qquad (36)$$

Then $$\phi_p = \frac{M_p}{EI} = \frac{\sigma_y Z}{EI}$$

$$= \frac{33 \times 47.1}{30 \times 10^3 \times 289.6} = 0.000179 \text{ rad./in.} \qquad (37)$$

Substituting in (36) for ϕ_p and L,

$H_B = 0.166 \times 0.000179 \times 360 = 0.0107$ rad.

$H_B = 0.61$ degrees

Therefore, a hinge angle of 0.61 degrees is required at the support to form a mechanism in a 14 WF 30 beam continuous over three 30 ft. spans and loaded with a side span load equal to half the intensity of the main span load.

b. Examples of Extreme Cases

In practical design cases, the side span load intensity would rarely be more than the main span load, and because there must be some dead load, would rarely be less than 25% of the main span load. If α is assumed to be bounded by these limits, $1.0 > \alpha > 0.25$, and Figs. 13 and 14 are searched for the greatest possible hinge angles, the following results are obtained:

Greatest Hinge Angle at Support

($\alpha = 0.25$, $\beta = 1.70$)

$H_B = 0.425\ \phi_p L$ (38)

Greatest Hinge Angle in Side Span Beam

($\alpha = 1.0$, $\beta = 1.85$)

$H_F = 0.186\ \phi_p L$ (39)

Greatest Hinge Angle in Main Span Beam
($\alpha = 0.25$ $\beta = 0.82$)

$$H_E = 0.030\ \phi p L \tag{40}$$

Again taking the case of a 30 ft. main span and a 14 WF 30, the maximum possible hinge angles are:

H_B = 0.0274 radians = 1.57 degrees

H_F = 0.0120 radians = 0.69 degrees

H_E = 0.00193 radians = 0.11 degrees

Thus, a much greater hinge angle is required if the first hinge is to form at a support than is required if the first hinge is to form at some intermediate location in a beam.

7.2 Comparison With Experimental Result

Data is available on the hinge rotation of a 14 WF 30 member tested in a corner connection test. (205C--T-101).[2] In this test, the moment gradient was nearly the same as it would be in the critical portion of a three-span continuous beam with $\alpha = 0.25$ and $\beta = 1.70$ (Fig. 15). At the same time, the member was subjected to an axial component of load. The hinge rotation measured over a 10 inch length was 0.0281 radians. This is greater than the 0.0274 radians which would be required for the beam in the example. Other sizes and shapes of test members have exhibited the same or better rotation characteristics. It thus appears that structural members should not have difficulty in developing the needed hinge angles at the supports of three-span continuous beams.

7.3 Comparison With Lateral Buckling Theory

A recent development in the theory on lateral buckling of members in the plastic range requires the knowledge of the hinge angles to determine the critical length of a member.[11] The method and the approximate methods derived from it are involved, so no numerical example will be given here. The indications are, however, that in cases where the moment gradient is very steep as is the case over the supports, there are favorable effects which reduce the tendency toward lateral buckling even though the required hinge angle may be quite large. In cases where the moment gradient is small as in the middle of the beams, there is a tendency toward lateral buckling under smaller hinge rotation angles. It is fortunate therefore that the hinge angles required in the middle of the spans will normally be quite small.

8. SUMMARY

The following summarizes the results and conclusions of this study of the rotation capacity of a three span continuous beam:

(1) Rotation capacity is the ability of a structural member to rotate at near-maximum moment.

(2) The hinge angle, H, (as distinguished from the virtual displacement angle, θ) is the required rotation of a given plastic hinge in a structure that is necessary to assure that the structure reaches ultimate load.

(3) The determination of the rotation capacity required in a structure is essentially the problem of calculating the hinge angle at the first plastic hinge at the instant that the structure has reached ultimate load.

(4) This report has discussed the calculation (by means of a modification of the slope-deflection method) of the rotation capacity required to form a mechanism in a structure loaded to its ultimate load--(Section 5).

(5) As an illustrative example, the method presented was used to obtain the magnitudes of hinge angles for a symmetrical three-span continuous beam. The structure considered had a center span length L, and two side spans of length βL. Uniformly distributed load of w lbs. per ft. was applied to the center span and αw lbs. per ft., to the side span. Expressing the side span loads and lengths in terms of α and β permitted general equations to be developed which covered a wide range of side span lengths and loads. The principal equations are summarized in the Appendix.

(6) The two possible types of mechanism which could form for this beam were determined, and an equation was developed to separate the values of α and β for which each would form (Eq. 4). The domains enclosing these values of α and β were depicted in graphical form (Fig. 2).

(7) Equations defining the location of the first plastic hinge were developed (Eq. 8,9) and the domains including the applicable values of α and β were given graphically (Fig. 3).

(8) Combining of the graphs for type of mechanism and location of the first plastic hinge gives a graph indicating four combinations of mechanism and first plastic hinge (Fig. 4).

(9) A detailed description of the behavior of a beam during the formation of a mechanism was given to aid in the visualization of hinge angles and virtual displacement angles. (Fig. 6-10).

(10) Expressions were developed for the hinge angles, H, for the four cases of failure mode. These are presented in Eq. 20, 27, 32, and 34, and in curve form in Figs. 13 and 14.

(11) The extreme values of possible hinge angles were determined from Fig. 13 and 14 and are as follows:

Maximum Hinge Angle at Interior Support

$$(\alpha = 0.25 \qquad \beta = 1.70)$$

$$H_B = 0.425\ \phi_p\ L \tag{38}$$

Maximum Hinge Angle in Side Span Beam

$$(\alpha = 1.0, \qquad \beta = 1.85)$$

$$H_F = 0.186\ \phi_p\ L \tag{39}$$

Maximum Hinge Angle in Main Span Beam

$$(\alpha = 0.25 \qquad \beta = 0.82)$$

$$H_E = 0.030\ \phi_p L \tag{40}$$

(12) For a specific extreme example of a three-span beam using a 14 WF 30 with a 30 ft. main span, the hinge angle required was 0.0274 radians. The result of a corner connection test, using a 14 WF 30 and having a moment diagram almost the same as the beam in the example gave a hinge rotation of 0.0281 radians. This was experimental evidence that the hinge angle requirements for three-span beams are not too severe to be met by rolled shapes. Since corner connections fabricated from other rolled shapes exhibited as good or better behavior it can be concluded that rolled shapes, in general, will exhibit satisfactory rotation capacity characteristics for three-span beams.

(13) The results of this study may be used to obtain hinge angles for use in lateral buckling and lateral bracing calculations (Ref. 11). The results indicate that the largest angles occur at interior supports where steep moment gradient and strain-hardening reduce the tendency toward lateral buckling. Usually, only small hinge angles are required in the spans where the flat moment gradient increases the tendency toward lateral buckling.

9. ACKNOWLEDGMENTS

The analytical work described in this report is part of a project on "Welded Continuous Frames and Their Components" being carried out under the direction of Lynn S. Beedle. The project is sponsored jointly by the Welding Research Council and the U. S. Navy Department under an agreement with the Institute of Research of Lehigh University. Funds are supplied by the American Institute of Steel Construction, American Iron and Steel Institute, Office of Naval Research, Bureau of Ships, and the Bureau of Yards and Docks. The work was done at Fritz Engineering Laboratory of which Professor William J. Eney is Director.

The original impetus for the study of the three span beam was provided through a discussion with E. R. Estes of A.I.S.C. who submitted the inequality shown as Eq. (8) defining the boundary between the formation of first plastic hinges at supports and in the main span.

The guidance and moral support of Dr. Lynn S. Beedle in discussing and reviewing this report are sincerely appreciated.

10. NOMENCLATURE

Symbols:

E	Young's modulus of elasticity
H	hinge angle
I	moment of inertia of cross section
L	length of main span
M	bending moment
M_{NF}	moment at near end of member
M_{FN}	moment at far end of member
M_p	plastic hinge moment
R	rotation of a chord between ends of a member
Z	fully plastic section modulus
l	length of a member or portion of a member (Variable)
w	uniformly distributed load per unit length of span
α	ratio of side span unit load to main span unit load
β	ratio of side span length to main span length
δ	deflection
ϵ	strain
ϕ	curvature of member
θ	slope of deflection curve
σ	stress
σ_y	yield strength of steel
ζ	ratio of distance to plastic hinge in side span to side span length

Capital Letter Subscripts in Slope Deflection Equations

Single letter ------ joint
Double letter ------- span
1st letter ----- near end
2nd letter ...... far end

Definitions:

Plastic Hinge	A yielded section of a beam which acts as if it were hinged, except that it has a constant restraining moment.
Hinge Angle	The required rotation of a given plastic hinge in a structure that is necessary to assure that the structure reaches the ultimate load.
Rotation Capacity	The ability of a structural member to rotate at near-maximum moment.
Mechanism	A system of members (and/or segments of members) that can deform at constant load. It is used in the special sense that all hinges are plastic hinges (except pin ends).
Plastification of cross section	The development of full plastic yield of the cross section.
Redistribution of Moment	A process in which plastic hinges form successively in a redundant structure until the ultimate load of the structure is reached. In the process, a new distribution of moments is achieved in which portions of the structure which are less highly-stressed in the elastic state subsequently reach the plastic hinge value. Redistribution is accomplished by rotation through the hinge angle of earlier-formed plastic hinges.

11. REFERENCES

1. Beedle, L.S.
   Thürlimann, B.
   Ketter, R.L.
   PLASTIC DESIGN IN STRUCTURAL STEEL 1955 Summer Course Lecture Notes, Lehigh University--AISC 1955.

2. Driscoll, G.C., Jr.
   Fisher, J.W.
   Schütz, F.W., Jr.
   EFFECT OF SIZE ON THE BEHAVIOR OF WELDED CORNER CONNECTIONS, Progress Report Y, Welded Continuous Frames and Their Components, Fritz Laboratory Report No. 205C, June 1957, (Unpublished).

3. Driscoll, G.C., Jr.
   Beedle, L.S.
   THE PLASTIC BEHAVIOR OF STRUCTURAL MEMBERS AND FRAMES, Progress Report No. 21, Welded Continuous Frames and Their Components. The Welding Journal, Research Suppl., June, 1957, page 275-s.

4. Haaijer, G.
   PLATE BUCKLING IN THE STRAIN HARDENING RANGE, ASCE Proceedings Paper 1212, April 1957.

5. Haaijer, G.
   Thürlimann, B.
   ON INELASTIC LOCAL BUCKLING IN STEEL, Presented at ASCE 1956 Annual Convention, Pittsburgh, Pa., October 1956.

6. Knudsen, K.E.
   Yang, C.H.
   Johnston, B.G.
   Beedle, L.S.
   PLASTIC STRENGTH AND DEFLECTIONS OF CONTINUOUS BEAMS, The Welding Journal, May 1953, page 240-s.

7. Symonds, P.S.
   A REVIEW OF METHODS FOR THE PLASTIC ANALYSIS OF RIGID FRAMES OF DUCTILE METAL, Tech. Rep. A 11-S6/86, Brown University to Office of Naval Research, May 1950, pp. 44-49.

8. Symonds, P.S.
   Neal, B.G.
   RECENT PROGRESS IN THE PLASTIC METHODS OF STRUCTURAL ANALYSIS, Journal of the Franklin Institute, 252 (5&6), 1951.

9. Sutherland, H.
   Bowman, H.L.
   STRUCTURAL THEORY, Fourth Edition, John Wiley and Sons, New York, 1950, p.242.

10. Toprac, A.A.
    Beedle, L.S.
    Johnston, B.G.
    CONNECTIONS FOR WELDED CONTINUOUS PORTAL FRAMES, Part I--"Test Results and Requirements for Connections", The Welding Journal 30(7) Research Suppl. 357-s, 1951. Part II--"Theoretical Analysis of Straight-Knees", Ibid., 30(8), Research Suppl. 397-s, 1951. Part III--"Discussion of Test Results and Conclusions", Ibid., 31(11), Research Suppl. 543-s, 1952.

11. White, M.W. THE LATERAL-TORSIONAL BUCKLING OF YIELDED STRUCTURAL STEEL MEMBERS, Ph.D. Dissertation, Lehigh University, 1956.

12. Yang, C.H., Beedle, L.S., Johnston, B.G. RESIDUAL STRESS AND THE YIELD STRENGTH OF STEEL BEAMS, Progress Report No. 5, Welded Continuous Frames and Their Components, The Welding Journal 31(4), Research Suppl. 205-s to 229-s (1952).

APPENDIX

Summary of Equations
(See Fig. 1 for nomenclature)

A. Plastic Hinge Moments

1. Main Span Mechanism

$$M_p = \frac{wL^2}{16} \tag{1}$$

2. Side Span Mechanism

$$M_p = \frac{\alpha\beta^2 wL^2}{11.66} \tag{2}$$

B. Limits

1. Between Main Span and Side Span Mechanisms

$$\alpha\beta^2 = 0.728 \tag{4}$$

2. Between First Hinge at B and E

$$\frac{\beta + 1.5}{\alpha\beta^3 + 1} = 2 \tag{8}$$

3. Between First Hinge at B and F

$$\frac{(3\alpha\beta^3 + 6\alpha\beta^2 - 1)^2}{\alpha\beta^2(2\beta + 3)(\alpha\beta^3 + 1)} = 8 \tag{9}$$

C. Hinge Angles

1. Main Span Mechanism--First Hinge at Support B

$$\frac{H_B}{\phi_p L} = \frac{2}{3}\alpha\beta^3 - \frac{1}{3}\beta + \frac{1}{6} \tag{27}$$

2. Main Span Mechanism--First Hinge in Span at E

$$\frac{H_E}{\phi_p L} = \frac{2}{3}\beta - \frac{1}{3} - \frac{4}{3}\alpha\beta^3 \tag{20}$$

3. Side Span Mechanism--First Hinge at Support B

$$\frac{H_B}{\phi_p L} = 0.1524\beta - \frac{1}{2} + \frac{0.486}{\alpha \beta^2} \qquad (32)$$

4. Side Span Mechanism--First Hinge in Span at F

$$\frac{H_F}{\phi_p L} = 0.368\beta - 1.207 + \frac{1.173}{\alpha \beta^2} \qquad (34)$$

FIGURES

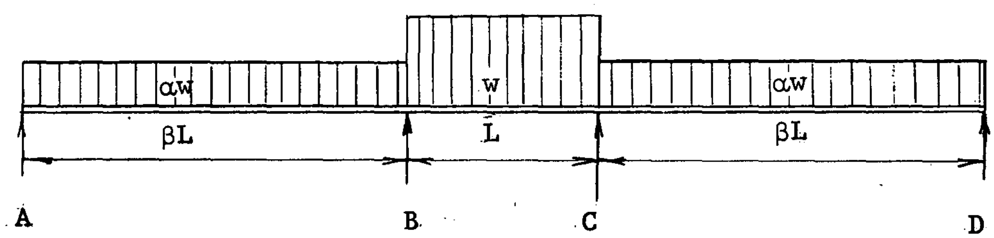

(a) Beam Dimensions and Loading

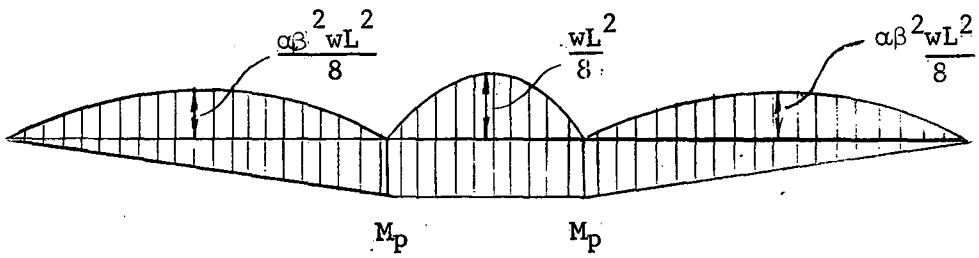

(b) Moment Diagram

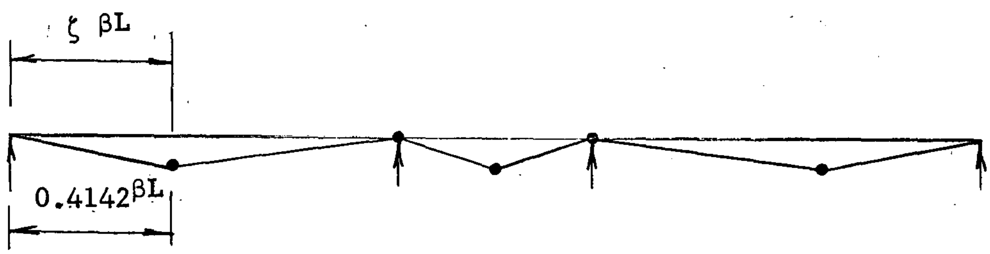

(c) Possible Mechanisms

Fig. 1 Beam Dimensions, Loading, Moment Diagram, and Possible Mechanisms

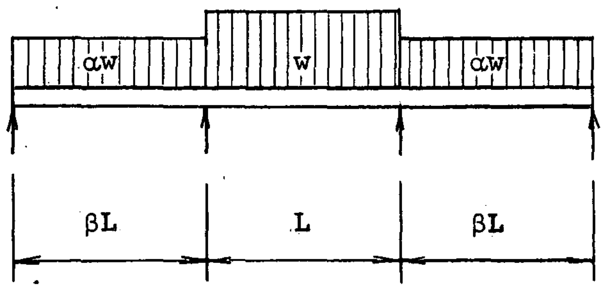

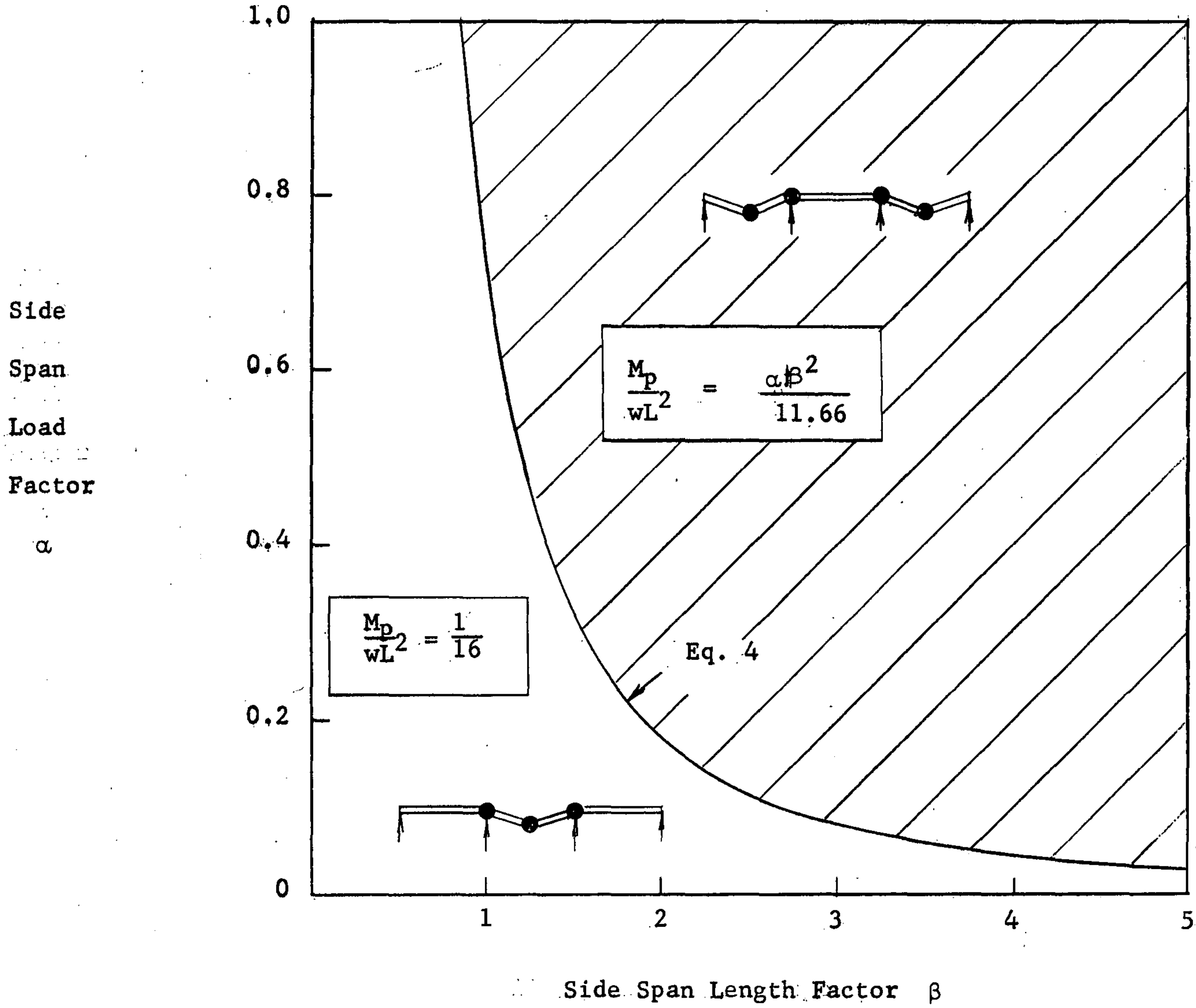

FIG 2 TYPE OF MECHANISM

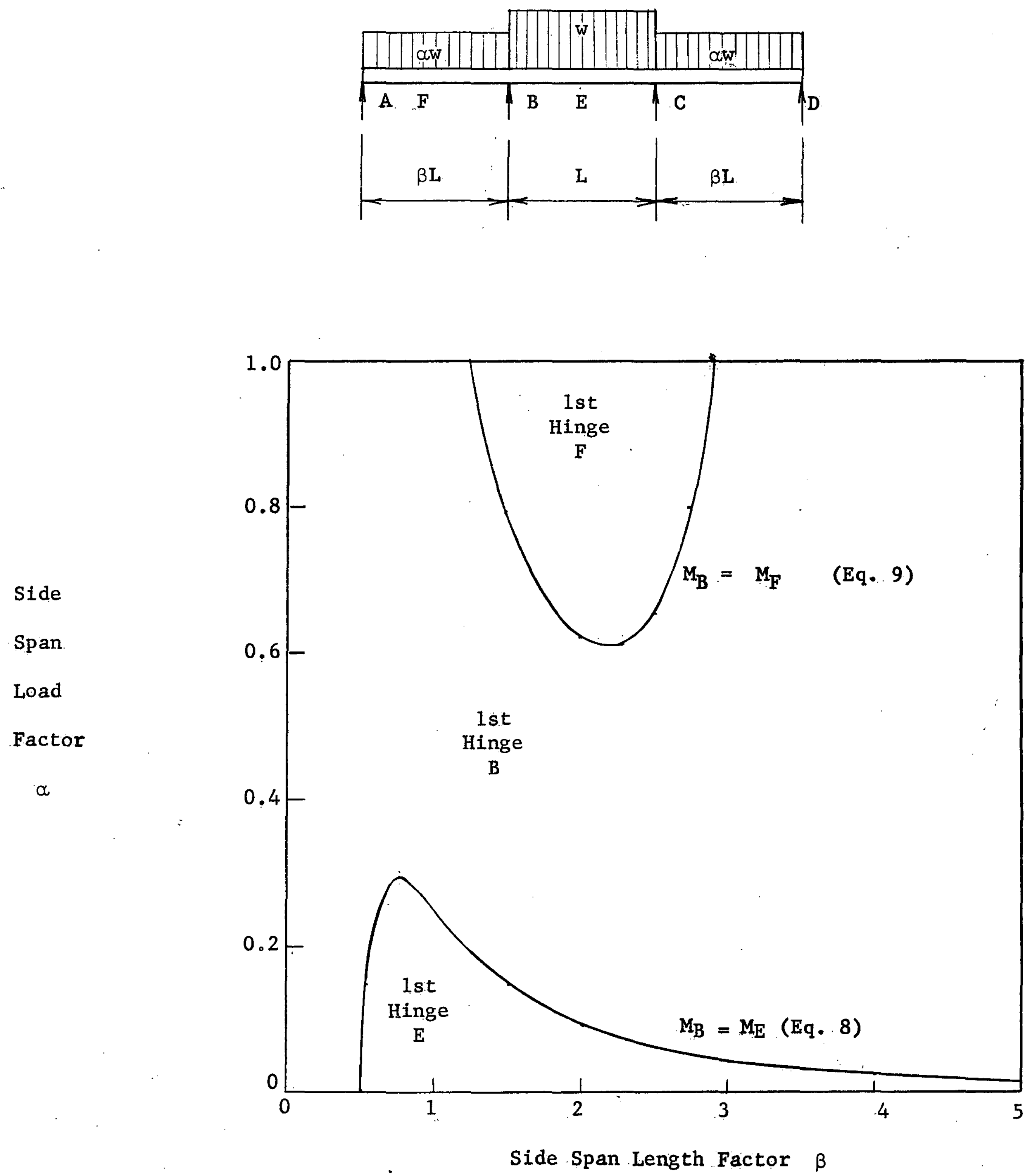

FIG. 3 LOCATION OF FIRST PLASTIC HINGE

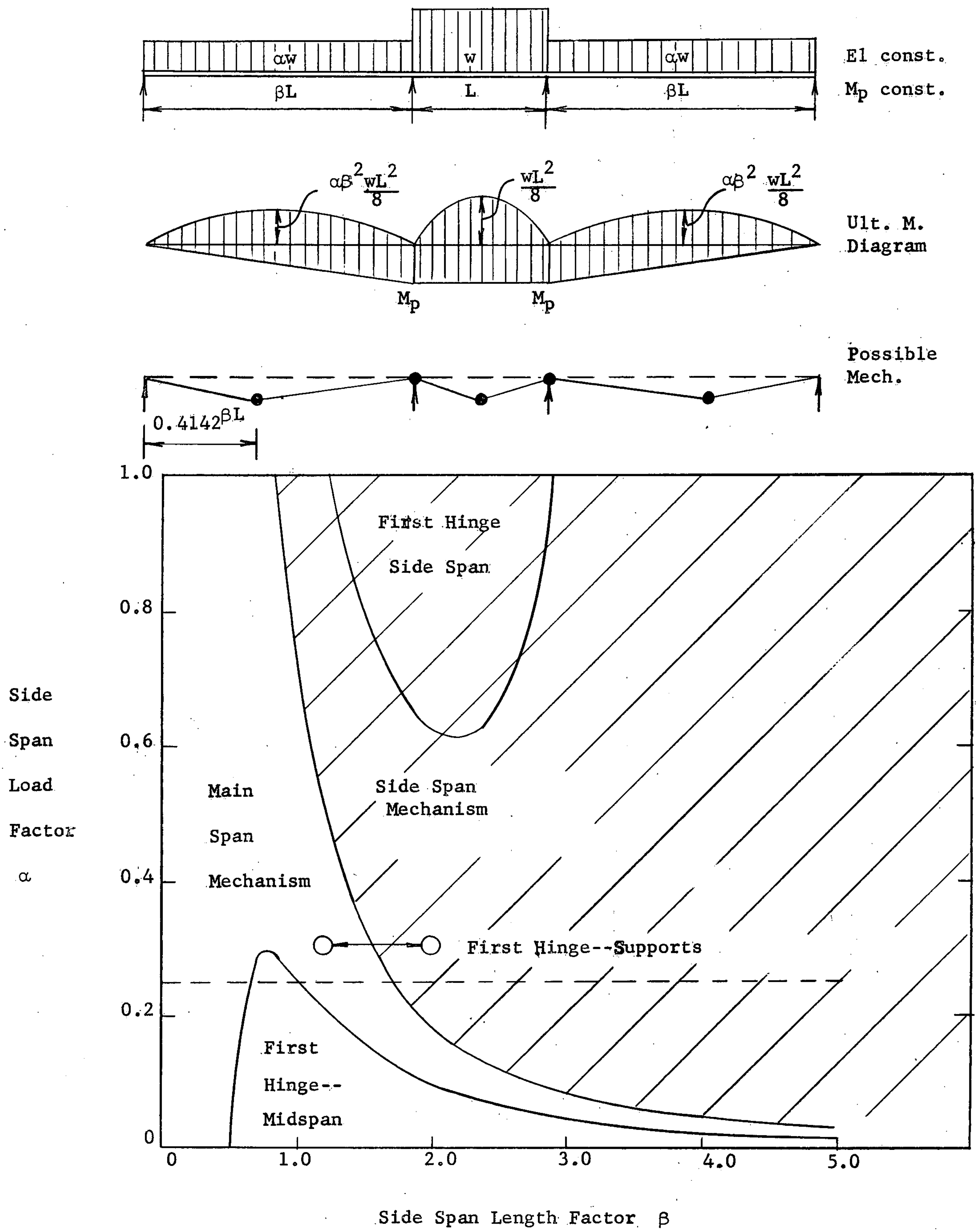

FIG. 4 LIMITS OF MECHANISMS

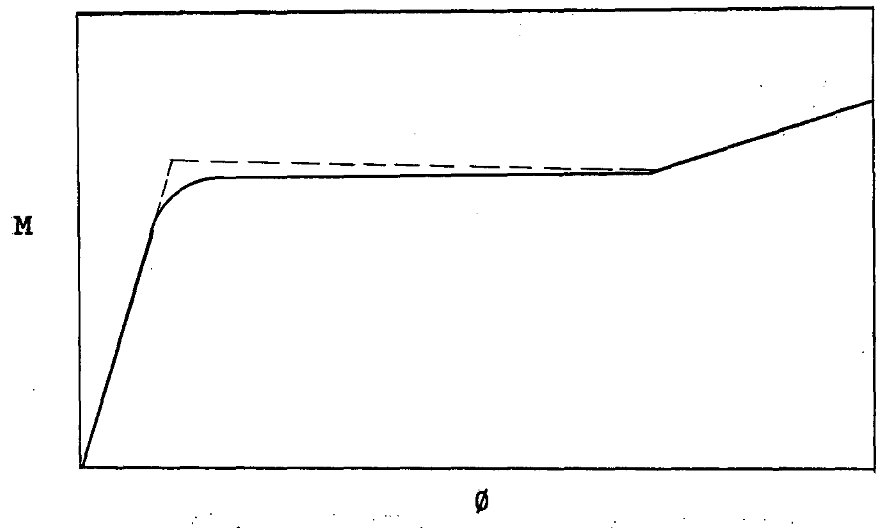

FIG. 5a. ACTUAL M-Ø CURVE FOR WF SHAPE

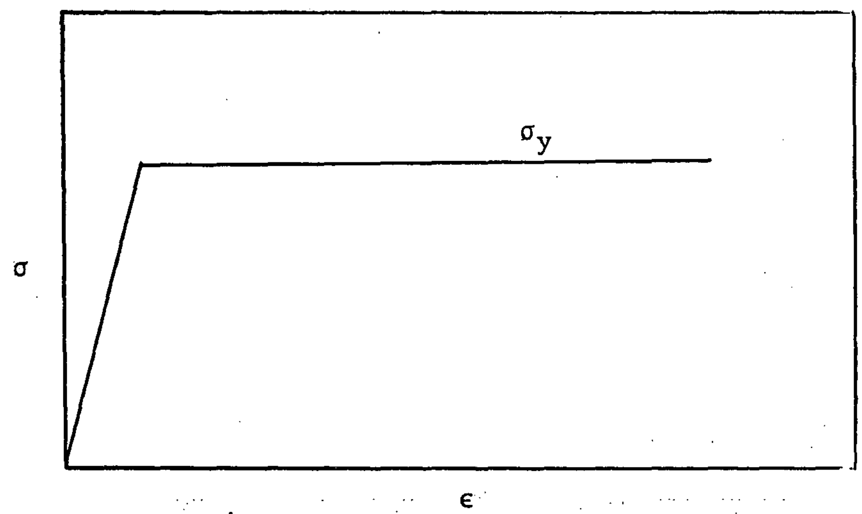

FIG. 5b. IDEALIZED STRESS-STRAIN CURVE

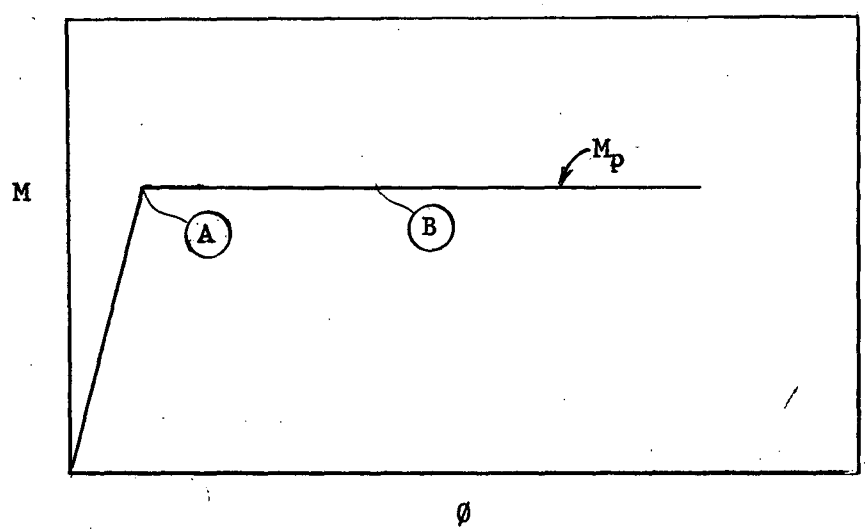

FIG. 5c. IDEALIZED M-Ø CURVE

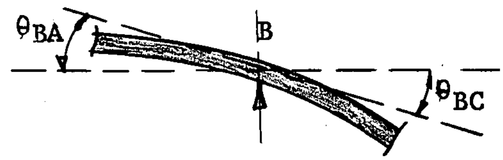

$\theta_{BA} = \theta_{BC}$

Elastic slope or slope prior to formation of plastic hinge

FIG. 6a

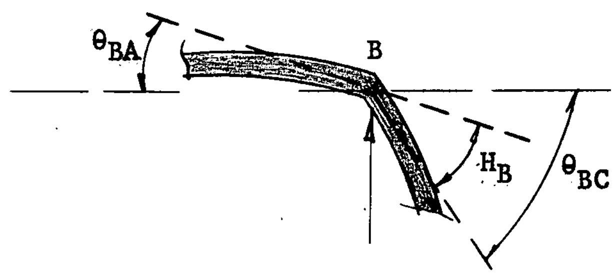

$\theta_{BA} \neq \theta_{BC}$

$H_B = \theta_{BC} - \theta_{BA}$

FIG. 6b

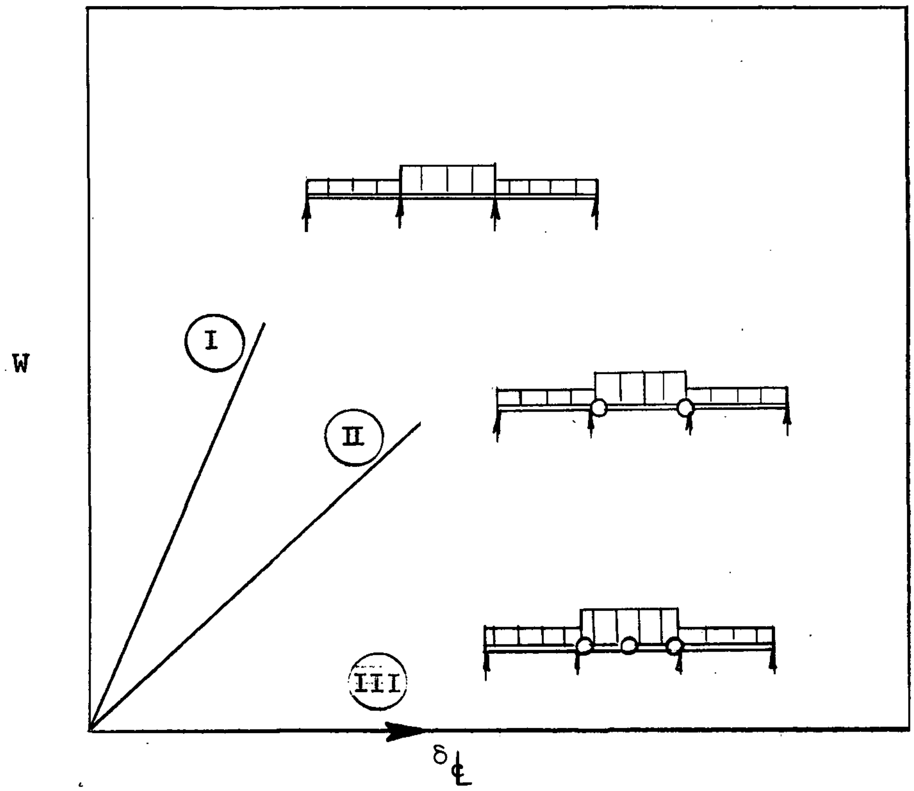

FIG. 7a INCREMENTAL BEHAVIOR OF BEAM FORMING A MECHANISM

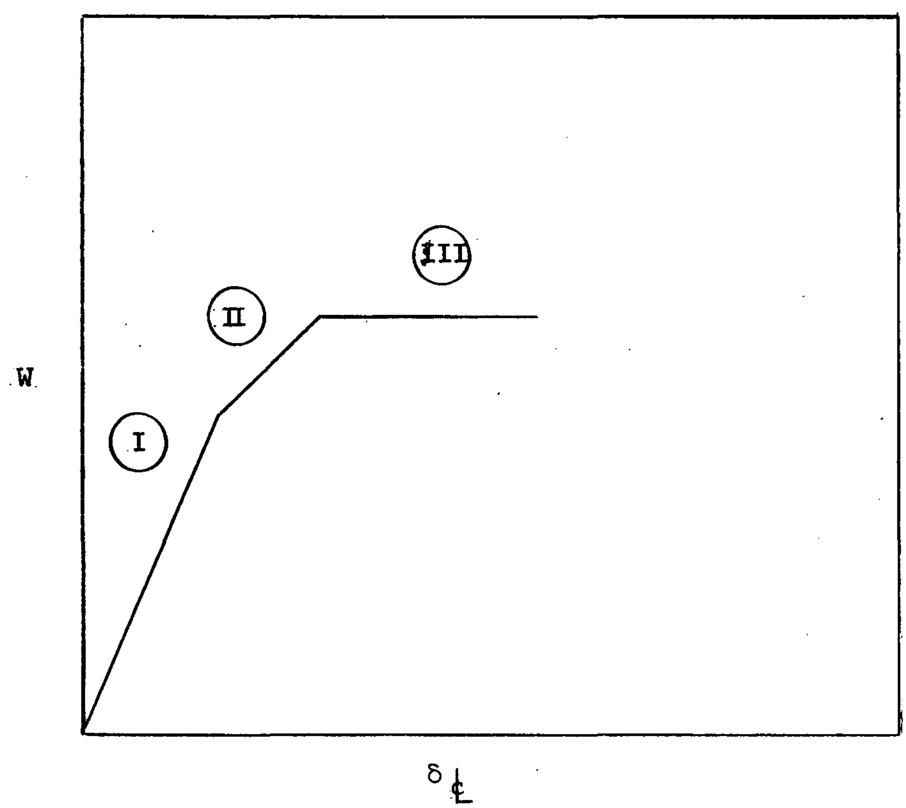

FIG. 7b TOTAL BEHAVIOR OF BEAM FORMING A MECHANISM

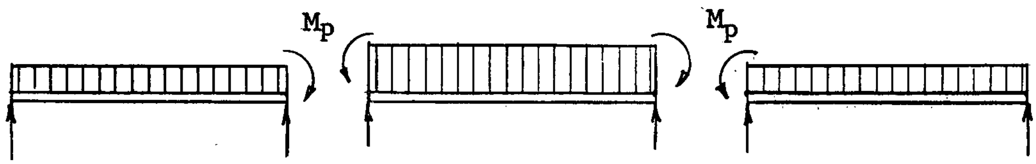

FIG. 8

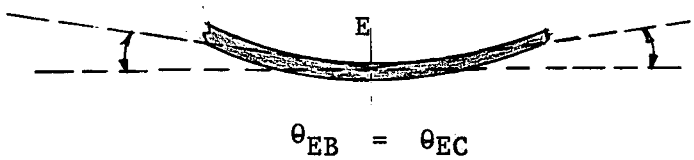

FIG. 9a

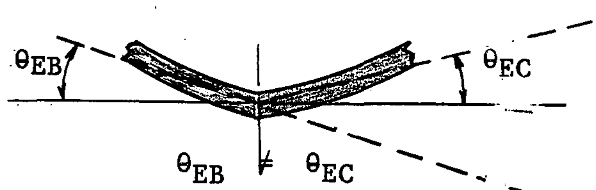

FIG. 9b

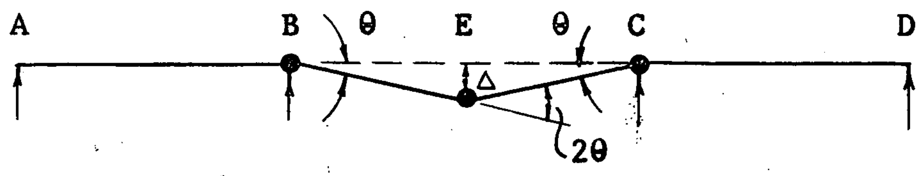

FIG. 10a

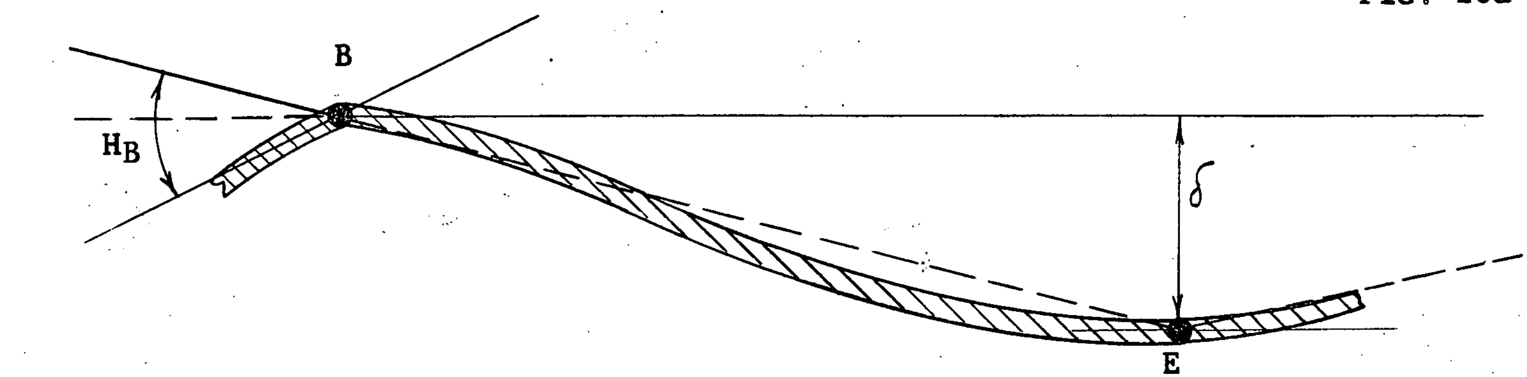

FIG. 10b

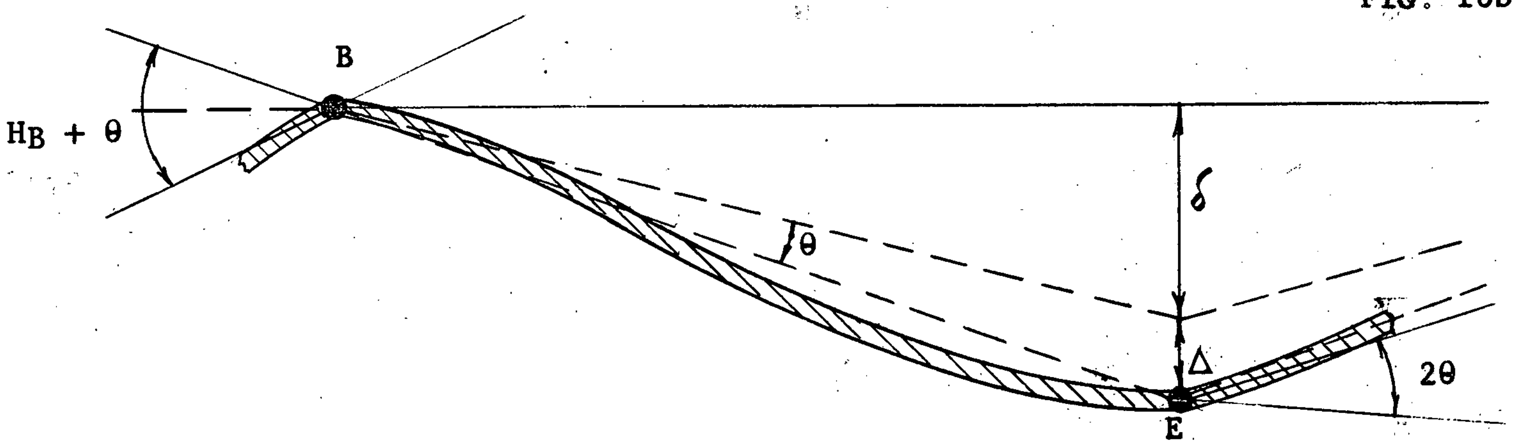

FIG. 10c

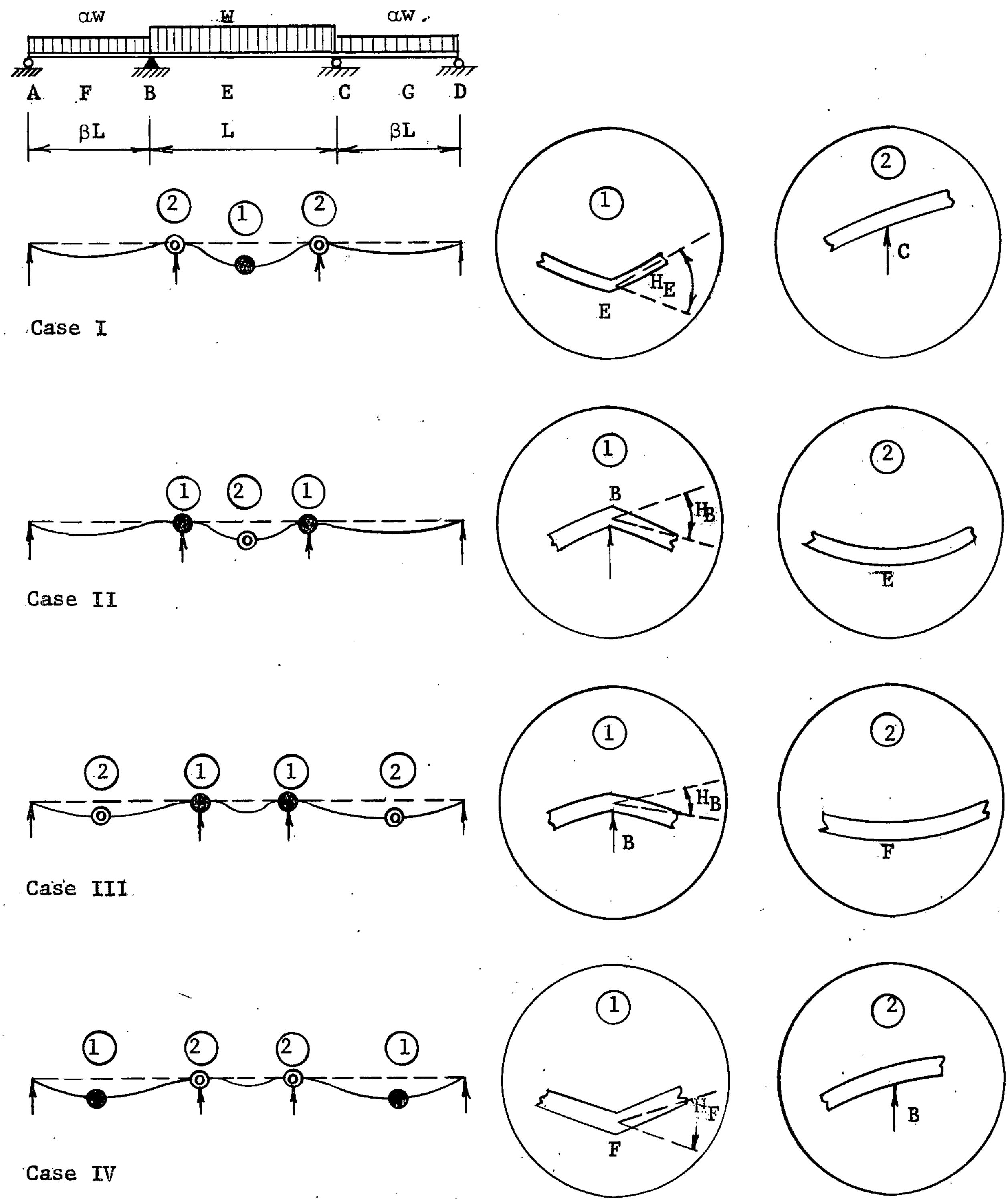

FIG. 11 POSSIBLE ORDER OF FORMATION OF PLASTIC HINGES

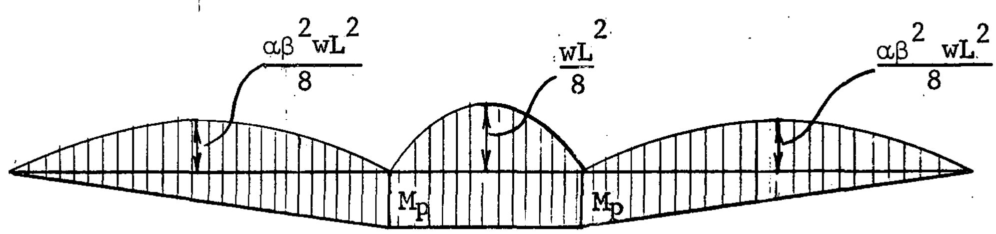

<u>Case I</u> First Hinge in Main Span

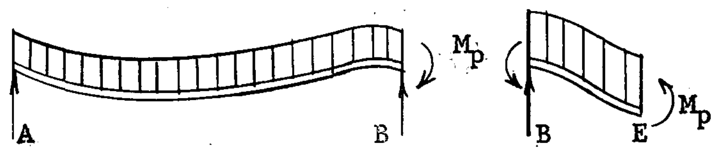

$\delta = 0$ | $\delta = 0$ | $\delta = ?$
$\theta = ?$ | $\theta_{BA} = \theta_{BE}$ | $\theta = ? = \theta_{EB}$
$M = 0$ | $M = M_p$ | $M = M_p$

<u>Case II</u> & <u>Case III</u> First Hinge at Interior Support

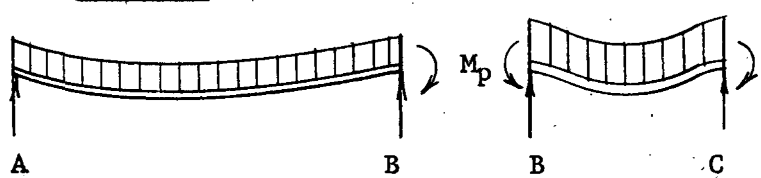

$\delta = 0$ | $\delta = 0$ | $\delta = 0$
$\theta = ?$ | $\theta = ? = \theta_{BA}$ | $\theta = ? = \theta_{BC}$
$M = 0$ | $M = M_p$ | $M = M_p$

<u>Case IV</u> First Hinge in Side Span

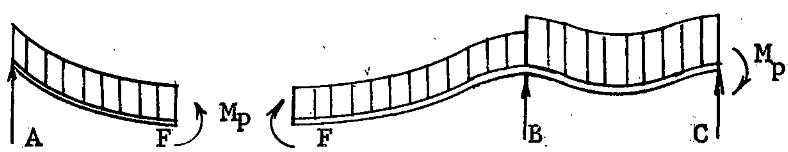

$\delta = 0$ | $\delta = ?$ | $\delta = ?$ | $\delta = 0$
$\theta = ?$ | $\theta = ? = \theta_{FA}$ | $\theta = ? = \theta_{FB}$ | $\theta_{BF} = \theta_{BC}$
$M = 0$ | $M = M_p$ | $M = M_p$ | $M = M_p$

FIG. 12 BOUNDARY CONDITIONS FOR CALCULATING HINGE ANGLES

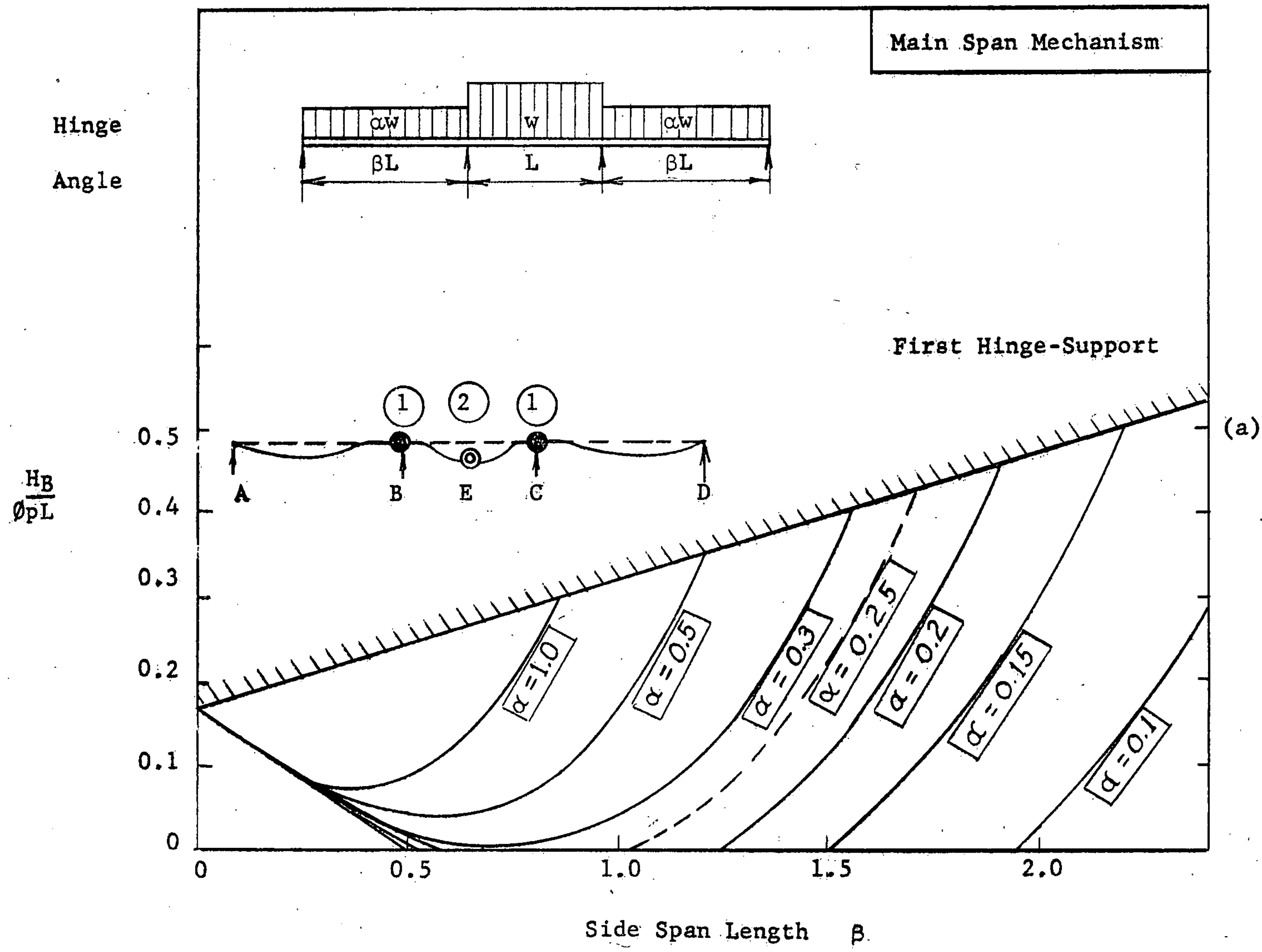

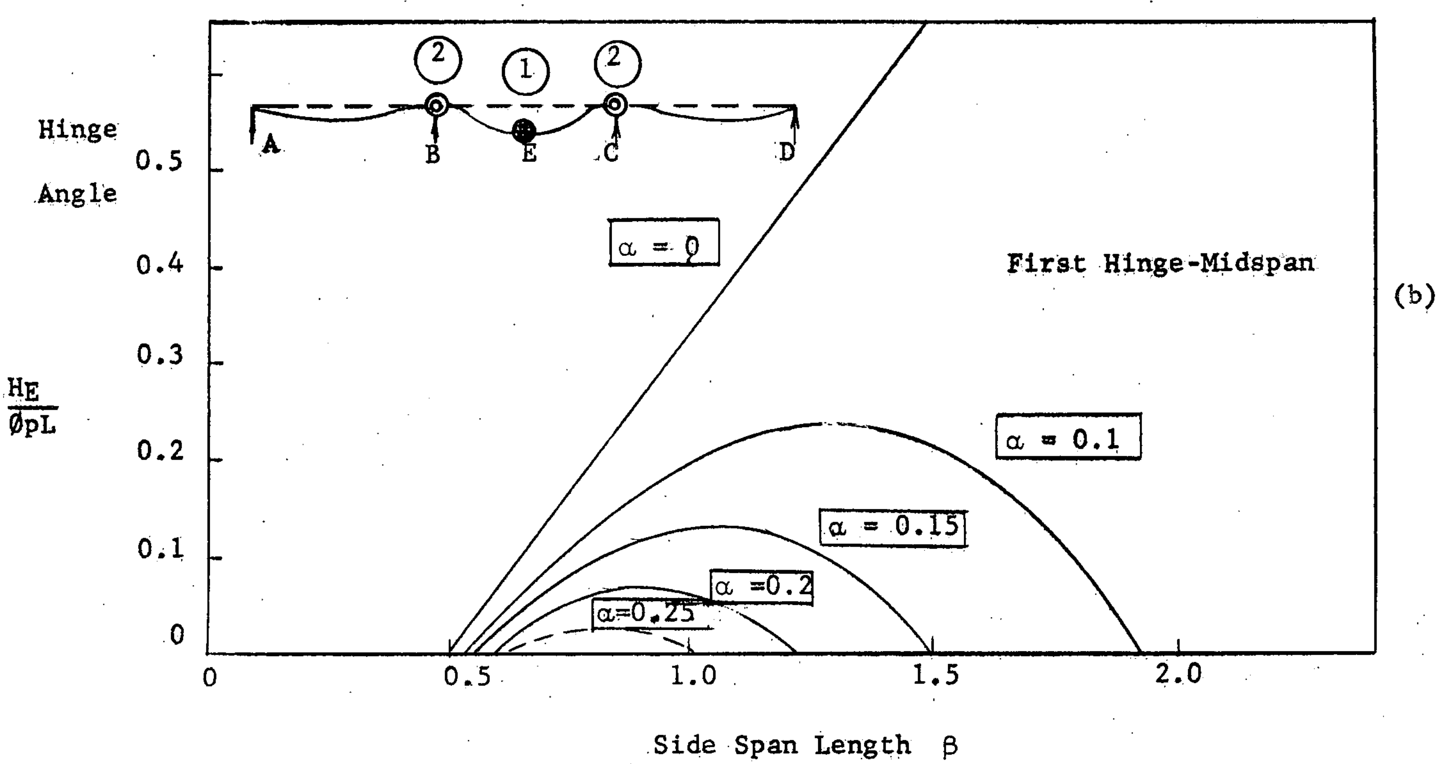

FIG. 13 HINGE ANGLES FOR MAINSPAN MECHANISM

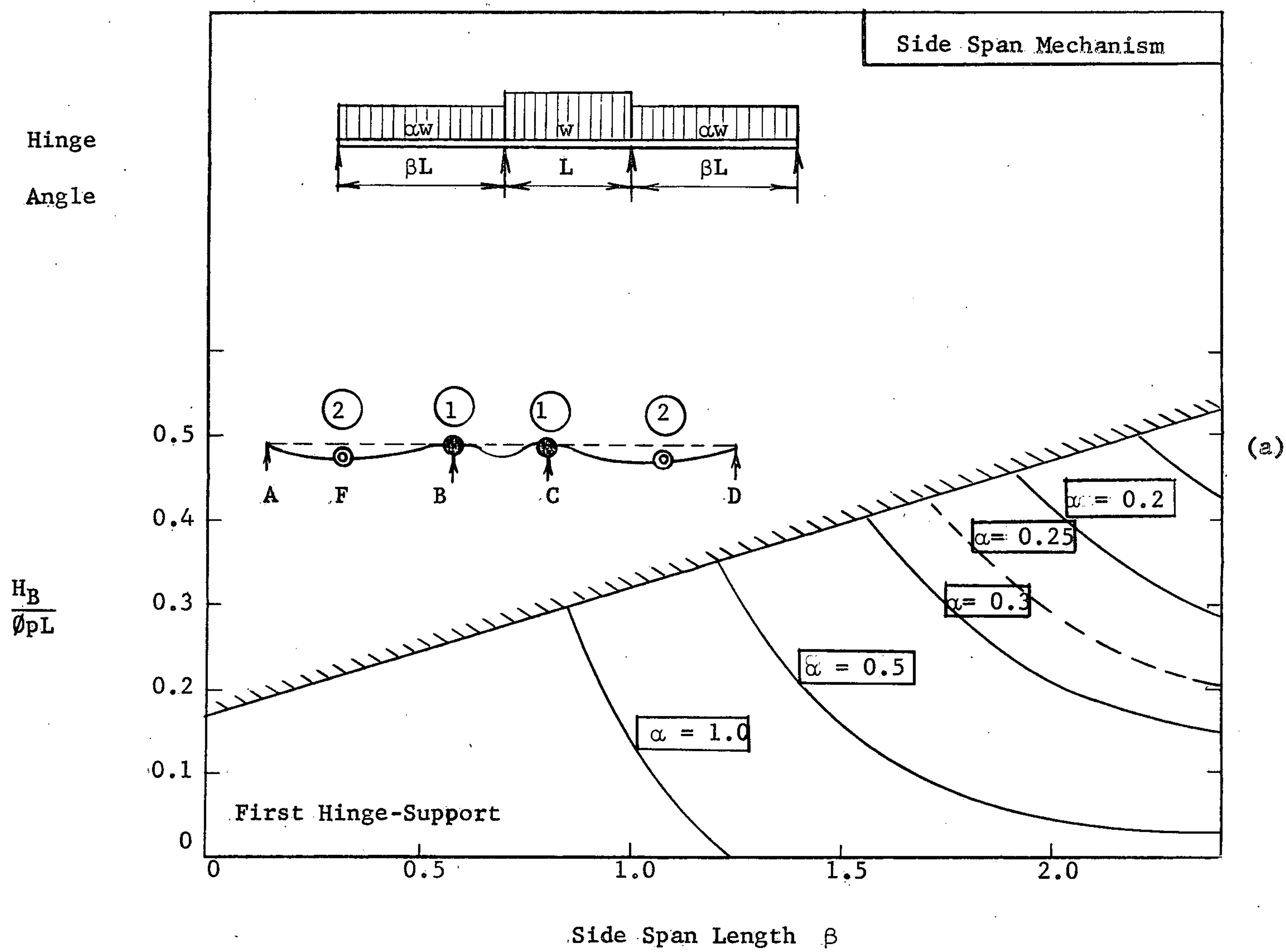

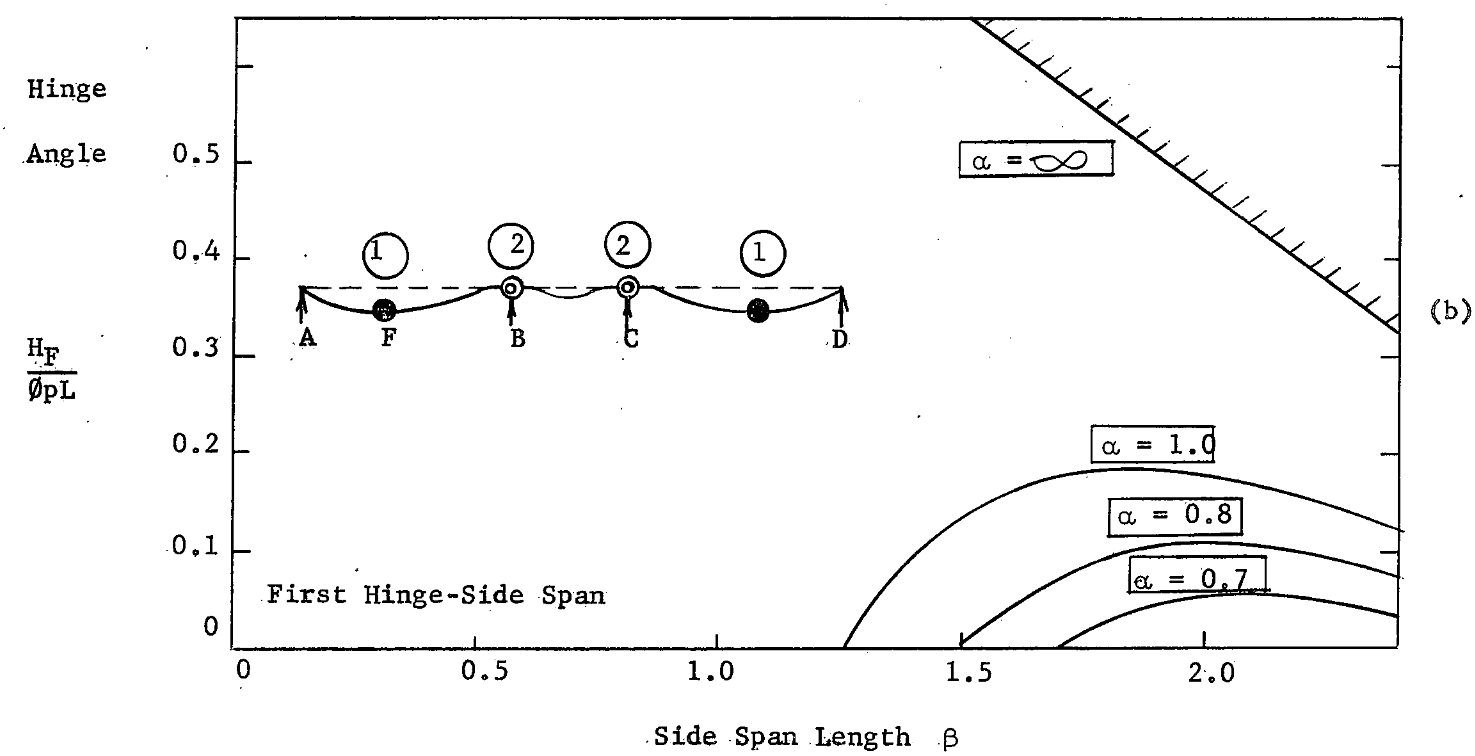

FIG. 14 HINGE ANGLES FOR SIDE SPAN MECHANISM

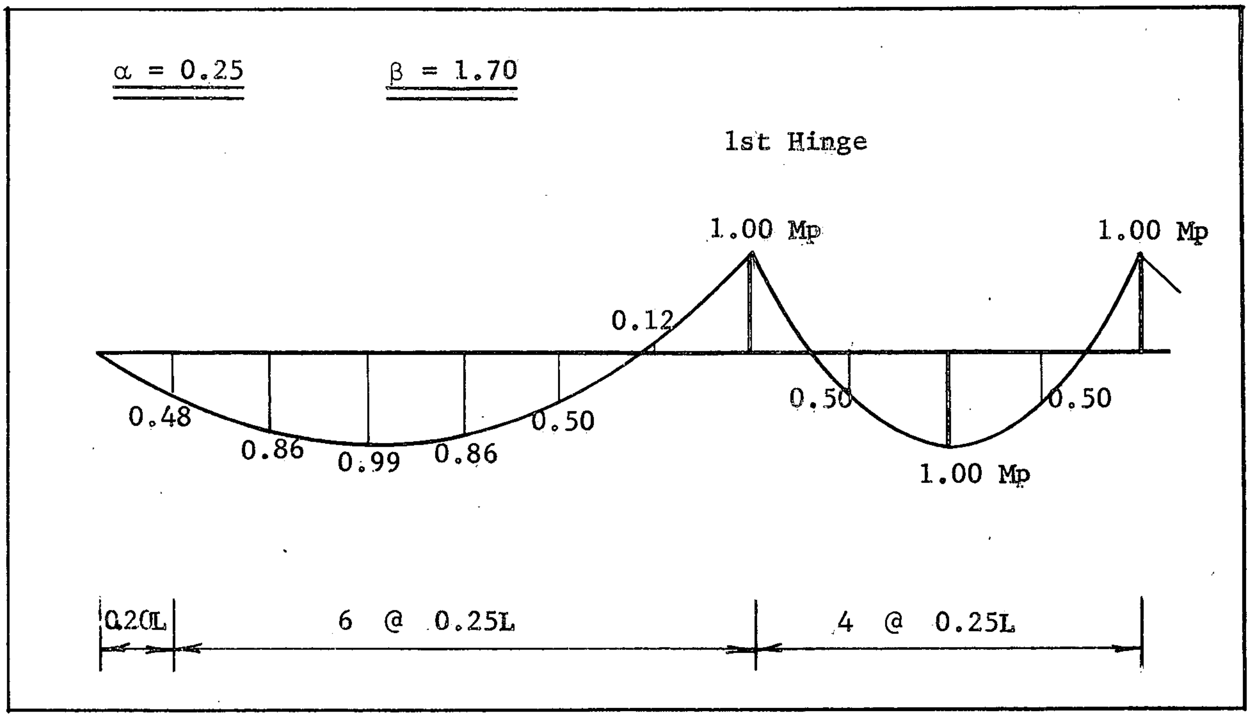

(a) Moment Diagram for Three-Span Beam (14WF30)

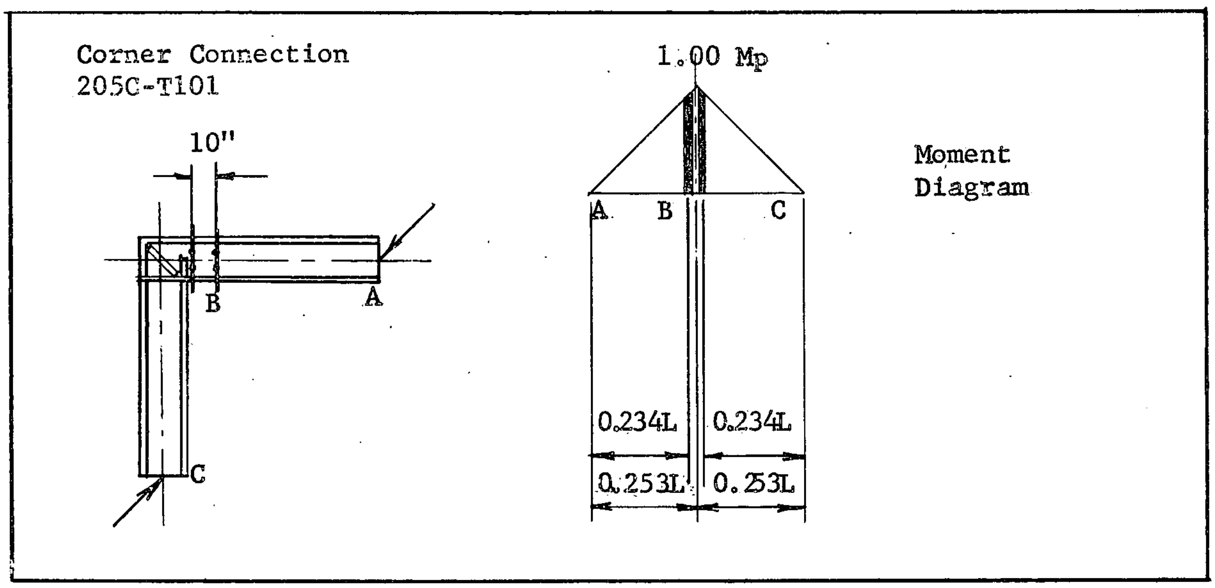

(b) Moment Diagram for Corner Connection (14WF30)

FIG. 15 COMPARISON OF MOMENT DIAGRAM FOR THEORETICAL EXAMPLE OF THREE-SPAN BEAM WITH MOMENT DIAGRAM FOR EXPERIMENTAL TEST OF CORNER CONNECTION